Dalton Transactions

ROYAL SOCIETY OF CHEMISTRY

PAPER

View Article Online
View Journal | View Issue

Cite this: *Dalton Trans.*, 2022, **51**, 8249

Synthesis, electronic nature, and reactivity of selected silylene carbonyl complexes†

Juliane Schoening,[a] Chelladurai Ganesamoorthy,[a] Christoph Wölper,[a] Ephrath Solel,[b] Peter R. Schreiner[b,c] and Stephan Schulz *[a,d]

Received 28th April 2022,
Accepted 2nd May 2022

DOI: 10.1039/d2dt01335e

rsc.li/dalton

Room-temperature stable main group element carbonyl complexes are rare. Here we report on the synthesis of two such complexes, namely gallium-substituted silylene-carbonyl complexes $[L(X)Ga]_2SiCO$ (X = I **2**, Me **3**; L = HC[C(Me)NDipp]$_2$, Dipp = 2,6-^{i}Pr$_2$C$_6$H$_3$) by reaction of three equivalents of LGa with $IDippSiI_4$ (IDipp = 1,3-bis(2,6-^{i}Pr$_2$C$_6$H$_3$)-imidazol-2-ylidene) or by salt elimination from $[L(Br)Ga]_2SiCO$ with MeLi. Both silylene carbonyl complexes were spectroscopically characterized as well as with single crystal X-ray diffraction (sc-XRD), while their electronic nature and the specific influence of the Ga-substituents X was evaluated by quantum chemical computations. In addition, we report the oxidative addition reaction of $[L(Br)Ga]_2SiCO$ with NH_3, yielding $[L(Br)Ga]_2Si(H)NH_2$ **4**, demonstrating the promising potential of such complexes for small molecule activation.

Introduction

Low-valent main group metal compounds with an energetically high lying HOMO and a low lying LUMO are electronically similar to transition metal complexes and therefore provide alternative approaches to reactions previously only possible with use of the latter.[1] In particular, monovalent group 13 diyls LM (M = Al, Ga) and divalent silylenes R_2Si: have proven to be promising reagents in small molecule activation,[2] *e.g.*, H_2, CO_2, ethylene, acetylene, and others, including catalytic processes.[3] One of the most typical reactions of transition metals is their capability to form stable carbonyl complexes: σ-donation of the CO electron lone pair (HOMO) into an empty acceptor orbital of the transition metal and π-backbonding from a filled *d*-orbital into the empty π* orbital (LUMO) results in the formation of a very strong metal–CO bond. In marked contrast, only a handful of stable main group element carbonyl complexes have been isolated, since main group elements typically do not have suitable orbitals for π-backbonding.[4] Matrix isolation experiments yielded a small number of main group element carbonyl complexes, including *s*-block metal complexes $M(CO)_8$ (M = Ca, Sr, Ba) as well as carbonyl ions of barium $Ba(CO)^q$ (q = 1+/1−),[5a,b] whose bonding situation has been controversially discussed,[5c,d] and boron $B(CO)_2^-$.[5e] In marked contrast, room-temperature stable carbonyl complexes only formed with strongly Lewis acidic boranes such as $(X_2B)_3BCO$ (X = F, Cl),[6a] $B(CF_3)_3$ **A**,[6b] and B_3H_7 **B**,[6c] respectively. In 2015, Braunschweig *et al.* reported the only dicarbonyl main group element complex known to date. Borylene dicarbonyl $TpB(CO)_2$ **C** (Tp = 2,6-Trip$_2$-C$_6$H$_3$, Trip = 2,4,6-^{i}Pr$_3$-C$_6$H$_2$), which releases CO upon irradiation as is known for transition metal carbonyl complexes, formed upon thermal treatment of a solution of $TpBCr(CO)_5$ under CO atmosphere.[7] Very recently, the same group isolated a carbene-stabilized boron-carbonyl complex LB(H)CO **D** that formed as an intermediate in the reaction of the carbene-coordinated diborene $L_2B_2H_2$ with CO_2 (Chart 1).[8a] However, due to the rather short B–C and long C–O bond, the electronic structure of **D** is better described as a borylketene, similar to aryl-substituted cAAC-bound arylborylenes LB(Ar)CO.[8b,c] The same is true for room-temperature stable sodium phosphaethynolate $[Na(OCP)(dme)_2]_2$[9] as well as group 13, 14, and 15 element phosphaketenes (R_2PPCO),[10] which serve as "masked" carbonyls since they react with release of CO in a variety of reactions.

In group 14 element chemistry, the synthesis of carbonyl complexes has been frequently attempted using carbene-type compounds. However, the reaction of carbenes R_2C: with CO yielded thermodynamically favoured ketenes rather than carbene-carbonyls adducts.[11] In contrast, silylenes reacted

[a]*Inorganic Chemistry, University of Duisburg-Essen, Universitätsstr. 7, 45141 Essen, Germany. E-mail: stephan.schulz@uni-due.de*
[b]*Institute of Organic Chemistry, Justus Liebig University, Heinrich-Buff-Ring 17, D-35392 Giessen, Germany*
[c]*Center for Materials Research (LaMa), Justus Liebig University, Heinrich-Buff-Ring 16, 35392 Giessen, Germany*
[d]*Center for Nanointegration Duisburg-Essen (Cenide), University of Duisburg-Essen, Carl-Benz-Straße 199, 47057 Duisburg, Germany*

†Electronic supplementary information (ESI) available: Detailed synthetic procedures, analytical data, NMR, IR, computational details and cif files. CCDC 2144415 (**1**), 2144416 (**2**), 2144417 (**3**) and 2144418 (**4**). For ESI and crystallographic data in CIF or other electronic format see DOI: **https://doi.org/10.1039/d2dt01335e**

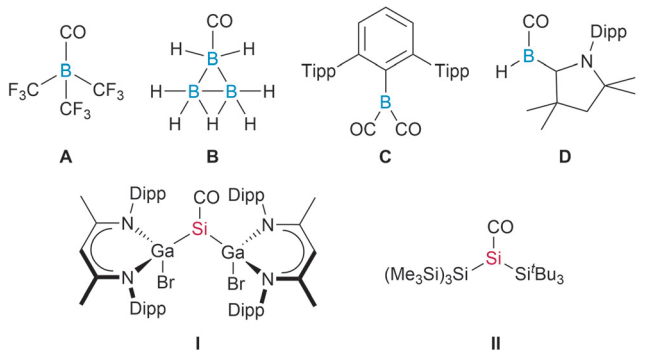

Chart 1 Selected *p*-block element carbonyl complexes stable at room temperature.

with CO with formation of silylene-carbonyl complexes R_2Si–CO, but these were so unstable that they could only be spectroscopically characterized in matrix isolation studies.[12] In remarkable contrast, room-temperature stable carbonyl complexes remained unknown, until very recently the Schulz and Inoue groups reported on the synthesis and single crystal X-ray structures of [L(Br)Ga]$_2$SiCO **I**[13] and [$(Me_3Si)_3Si$](^{t}Bu_3Si)SiCO **II**,[14] respectively. The use of sterically demanding and electron-rich silylenes, which was achieved by introducing L(Br)Ga and ^{t}Bu_3Si ligands to the central Si atom, turned out to be crucial for the generation of these carbonyl complexes. Quantum chemical computations revealed that CO serves as an electron donor to the silylene, forming a σ-C–Si bond, while the presence of the L(Br)Ga (**I**) and silyl substituents (**II**) increase the electron density at the silicon atom, enabling the π-backbonding to the π*-orbital of the CO, resulting in a bonding motif similar to that of transition metal carbonyl complexes.[13,14] Andrada *et al.* further pointed to an additional π back donation contribution from the HOMO−1 σ_{GaSi} orbital into the π^*_{CO} orbital in [L(Br)Ga]$_2$SiCO **I**. With stronger σ-donating substituents, this contribution was found to increase to up to 20% of the total orbital interaction.[15]

We now report on the syntheses and solid-state structures of two additional silylene carbonyl complexes [L(X)Ga]$_2$SiCO (X = I **2**, Me **3**) using alternative synthetic methods, and the influence of different substituents X (X = F, Cl, Br, I, Me, OMe, NMe_2) on their electronic structures is shown. In addition, reactions of [L(Br)Ga]$_2$SiCO **I** and ([L(Me)Ga]$_2$SiCO **3** with H_2, NH_3, and other reagents ($LiAlH_4$, $SnCl_4$) is compared. [L(Br)Ga]$_2$SiCO **I** was found to react *via* oxidative addition with all reagents including NH_3, yielding [L(Br)Ga]$_2$Si(H)NH_2 **4**, whereas complex **3** failed to react, illustrating the distinct role of the substituent X on the chemical reactivity of such silylene carbonyl complexes.

Results and discussion

Silicon tetrahalides SiX_4 (X = Cl, Br, I) differently react with LGa (Scheme 1) due to the different Si–X bond strengths. Oxidative addition reactions of LGa with SiX_4 (X = Cl, Br) in 1 : 1 and 2 : 1 molar ratios yielded L(X)GaSiX_3 (X = Cl,[16] Br[13]) and [L(X)Ga]$_2$SiX_2 (X = Cl,[17] Br[13]), but only [L(Br)Ga]$_2$SiBr_2 reacted with LGa to {[L(Br)Ga]Si[Ga(Br)][CHC(Me)NAr][C(Me)NAr]}.[13] Analogous reactions of SiI_4 failed to give [L(I)Ga]SiI_3 and [L(I)Ga]$_2$SiI_2, but {[L(I)Ga]Si[Ga(I)][CHC(Me)NAr][C(Me)NAr]} (**1**) was isolated from the reaction in a 3 : 1 molar ratio. In addition, only [L(Br)Ga]$_2$SiBr_2 reacted with LGa under CO atmosphere to [L(Br)Ga]$_2$SiCO **I**,[13] whereas any attempts to reduce [L(Cl)Ga]$_2$SiCl_2 under CO atmosphere with a variety of reducing agents, *e.g.*, Na, K, KC_8, L_2Mg_2, and LGa, respectively, as well as to react SiI_4 with three equivalents of LGa under CO atmosphere failed to give the desired silylene carbonyl complexes [L(Cl)Ga]$_2$SiCO and [L(I)Ga]$_2$SiCO (**2**). In marked contrast, the reaction of the carbene adduct IDippSiI_4 with three equivalents of LGa under CO atmosphere gave [L(I)Ga]$_2$SiCO (**2**) in reasonable yield (Scheme 1).

The ^{1}H NMR and ^{13}C NMR spectra of **1** and **2** are similar to those of analogous Br-substituted compounds **I** and **III**.[13] The ^{1}H NMR spectrum of **2** shows a singlet at 5.02 ppm of the γ-H proton, while the $^{13}C\{^1H\}$ NMR spectrum shows a signal at

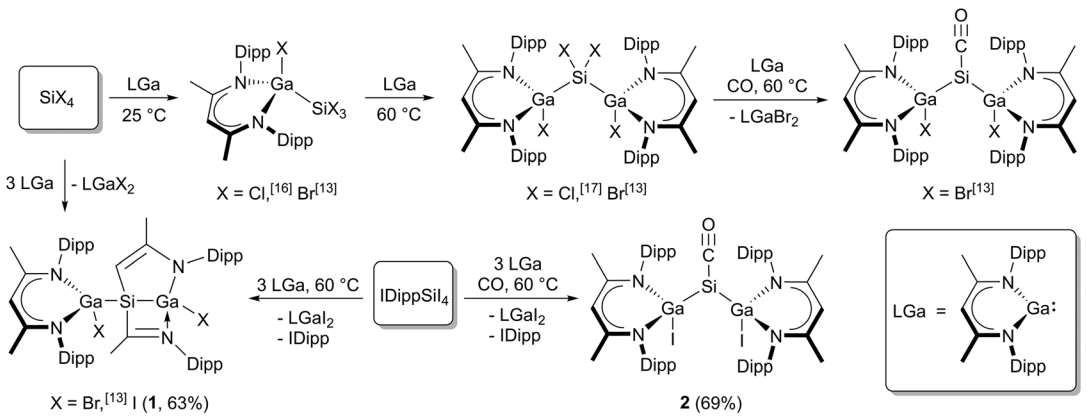

Scheme 1 Overview of reactions of SiX_4 (X = Cl, Br, I) or IDippSiI_4 with LGa in different molar ratios (1 : 1 to 1 : 3) including the synthesis of new complexes (**1**) and (**2**).

207.0 ppm for the CO group. The resonance in the $^{29}Si\{^1H\}$ NMR at −249.9 ppm is slightly shifted to higher field compared to that of $[L(Br)Ga]_2SiCO$ **I** (−256.5 ppm).[13] The IR spectrum of **2** exhibits a strong absorption band at 1934 cm^{-1}, which is shifted to a lower wavenumber compared to $[L(Br)Ga]_2SiCO$ **I** (1945 cm^{-1}).[13] These experimental findings indicate a slightly stronger π-backbonding contribution in **2**.

To study the influence of the ligand X in $[L(X)Ga]_2SiCO$ on their electronic nature, we became interested in replacing the electron-withdrawing (–I effect) halide substituents X (X = Br, I) by electron-donating (+I effect) alkyl groups, but unfortunately, LGa failed to oxidatively add Si–C bonds. Me/halide exchange reactions of $[L(X)Ga]_2SiCO$ (X = Br **I**, I **2**) with $AlMe_3$ and MeMgBr also failed, but salt elimination reaction of **I** with MeLi gave $[L(Me)Ga]_2SiCO$ **3** in 63% yield (Scheme 2). Any further attempts to introduce other substituents X (X = OMe, NMe_2) by salt elimination using the corresponding alkaline metal salt MX (M = Na, Li) to electronically modify the carbonyl complexes $[L(X)Ga]_2SiCO$ remained unsuccessful.

Carbonyl complexes **2**, **3**, and **I** form stable solutions in benzene and toluene at ambient temperature, whereas only complex **3** is stable in polar solvents such as CH_2Cl_2. $[L(Me)Ga]_2SiCO$ **3** is also thermally far more stable ($T_{dec.}$ = 249 °C) than complexes **2** ($T_{dec.}$ 168–169 °C) and **I** ($T_{dec.}$ 176–177 °C), indicating a stronger Si–CO bond due to a larger π backbonding character of $[L(Me)Ga]_2Si$ compared to $[L(X)Ga]_2Si$ (X = Br, I), respectively. This is confirmed by IR spectroscopy, since **3** shows a strong stretching vibration of the CO group at 1906 cm^{-1}. $[(Me_3Si)_3Si]({}^tBu_3Si)SiCO$ **II** shows an almost identical adsorption frequency (1908 cm^{-1}),[14] whereas those of **2** (1934 cm^{-1}) and **I** (1945 cm^{-1}) are blueshifted.

The ^1H NMR spectrum of **3** is similar to those of **2** and **I** and only shows an additional singlet at 0.32 ppm due to the Me group. The $^{13}C\{^1H\}$ NMR spectrum of **3** shows a resonance at 207.5 ppm (CO group), which is comparable to that observed for **I** (δ 206.5) and **2** (δ 207.0) but is shifted to higher field compared to $[(Me_3Si)_3Si)({}^tBu_3Si)SiCO$ **II** (226.1 ppm). In contrast, the singlet at −285.2 ppm in the $^{29}Si\{^1H\}$ NMR spectrum of **3** is shifted to higher field compared to **2** (−249.9 ppm), **I** (−256.5 ppm), and **II** (−228.5 ppm), respectively.

$[L(Br)Ga]_2SiCO$ **I** was shown to react as masked silylene.[13] To reveal the influence of the substituent X, we compared reactions of $[L(Br)Ga]_2SiCO$ **I** and $[L(Me)Ga]_2SiCO$ **3**, which contain the most electronegative (X = Br) and most electropositive (X = Me) substituent. Due to the larger π-backbonding contribution in **3** as was proven by the stronger redshift in the IR spectrum of **3**, complex **3** was expected to be less reactive than complex **I**.

Complexes **I** and **3** both react with two equivalents of $SnCl_4$ at ambient temperature with oxidation and almost quantitative formation of $[L(Cl)Ga]_2SiCl_2$ (Fig. S22, S23†). The formation of $[L(Cl)Ga]_2SiCl_2$ reflects the greater stability of Sn(II) *vs.* Si(II), and the Br/Cl and Me/Cl exchange at the Ga centers is also not unexpected due to the thermodynamically favored Ga–Cl bond. In contrast, only complex **I** reacted with H_2, $LiAlH_4$, and PBr_3 to $[L(Br)Ga]_2SiH_2$ and $[L(Br)Ga]_2SiBr_2$,[13] respectively, whereas complex **3** failed to react even at elevated temperatures (120 °C). Only LGa was formed in the reaction of **3** with H_2 after several days and identified by *in situ* ^1H NMR spectroscopy (Fig. S21†). These findings prove the reduced reactivity of carbonyl complex **3** compared to complex **I** most likely resulting from the more strongly bound CO group in **3**. We also reacted complexes **I** and **3** with NH_3 since silylenes are known to activate the rather strong N–H bond,[18] *i.e.,* Inoue's bis(silyl)silylene reacted already at −80 °C. **I** immediately reacted with NH_3 at −20 °C (Scheme 3) to $[L(Br)Ga]_2Si(H)NH_2$ **4**, whereas **3** did not react even at elevated temperatures up to 70 °C. Removal of unreacted NH_3 after several minutes is crucial to avoid the formation of a complex mixture of yet unidentified products, as was reported by *Inoue* and coworkers.[19]

The ^1H NMR spectrum of compound **4** shows a triplet at 4.67 ppm (Si–H) and a doublet at −1.67 ppm (NH_2), which are both in comparable regimes to previously reported complexes formed in NH_3 activation reactions (Si–H: 4.72–5.22 ppm; NH_2 –0.05 to 0.99 ppm).[18] In addition, the ^1H and ^{13}C NMR spectra of **4** show typical resonances of the β-diketiminate ligand. The N–H stretching bands of **4** in the IR spectrum at 3428 and 3345 cm^{-1} are close to those of previously reported compounds, as is also true for the Si–H stretching band at 2060 cm^{-1}.[18]

Single crystals of compounds **1–3** were obtained from benzene solutions upon storage at 4 °C for 72 h (**1**) and 24 h (**2**, **3**) or from toluene solution upon storage at −18 °C (**4**). Complexes **1–3** crystallize in the triclinic space group $P\bar{1}$ with one molecule in the asymmetric unit, and **4** in the monoclinic space group $C2/c$ (Fig. 1) with the molecule placed on a special position (twofold rotational axis). The Ga–Si (2.3805(9) Å; 2.3599(9) Å) and Si–C (1.849(3) Å, 1.932(3) Å) bond lengths in **1** are almost identical to the Ga–Si (2.3919(7) Å; 2.3628(7) Å) and Si–C bond lengths (1.864(2) Å, 1.939(2) Å) reported for {[L(Br)Ga]Si[Ga(Br)][CHC(Me)NDipp][C(Me)NDipp]}.[13] The Ga–Si

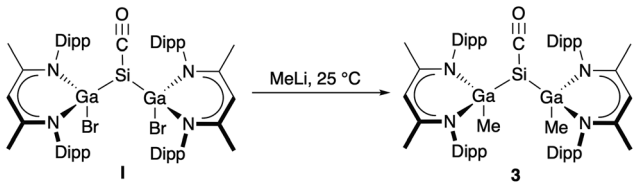

Scheme 2 Synthesis of $[L(Me)Ga]_2SiCO$ (**3**).

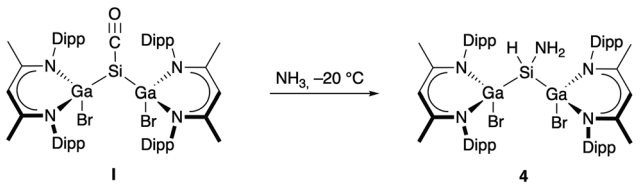

Scheme 3 Synthesis of $[L(Br)Ga]_2Si(H)NH_2$ (**4**).

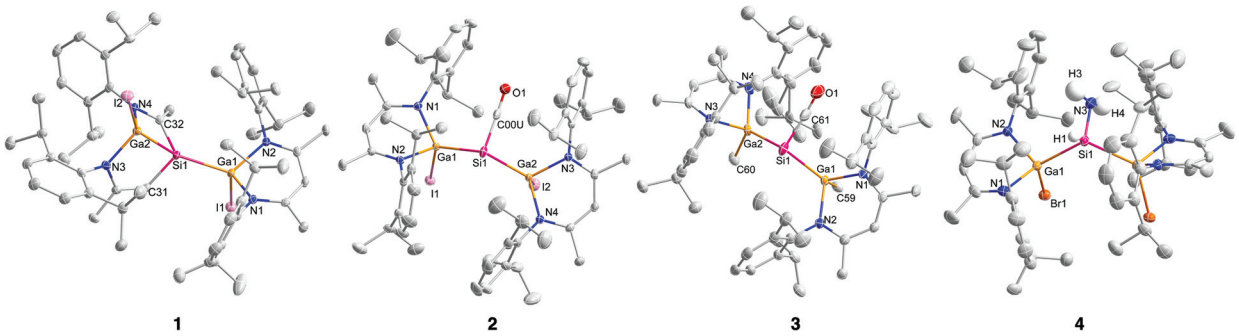

1 2 3 4

Fig. 1 Molecular structures of {[L(I)Ga]Si[Ga(I)][CHC(Me)NDipp][C(Me)NDipp]} (**1**), $[L(I)Ga]_2SiCO$ (**2**), $[L(Me)Ga]_2SiCO$ (**3**), and $[L(Br)Ga]_2Si(H)NH_2$ (**4**); ellipsoids set at 50% probability level; hydrogen atoms (except SiH and NH_2 in **4**) and solvent molecules (benzene) are omitted for clarity.

bond lengths in $[L(I)Ga]_2SiCO$ **2** (2.4230(8) Å, 2.4348(9) Å) and $[L(Me)Ga]_2SiCO$ **3** (2.4314(4) Å, 2.4213(4) Å) are similar to those in $[L(Br)Ga]_2SiCO$ **I** (2.4204(5) Å), whereas the Si–C bond lengths in **2** (1.808(9) Å) and **3** (1.770(2) Å) are much shorter than those of complexes **I** (1.865(6) Å) and **II** (1.794(2) Å), respectively (Table 1).

The Si–C bond length in **3** is also substantially shorter than Si–C single bonds (1.87–1.93 Å)[20] and close to Si–C double bond distances, which range from 1.70 to 1.76 Å.[20] These structural parameters indicate a higher π-backbonding contribution from the filled silicon sp^2 orbital to the π^*_{CO} antibonding orbital, probably resulting from the more electropositive character of the iodine and methyl groups compared to the bromine substituent in complex **I**, resulting in a slightly higher electron density at the silicon center. The elongated C–O bond lengths in **2** (1.149(3) Å) and **3** (1.144(2) Å) compared to that in **I** (1.136(7) Å) agrees with this description. Complex **II** showed an even longer C–O bond of 1.153(2) Å.

The Ga and Si atoms in silane complex $[L(Br)Ga]_2Si(H)NH_2$ **4** feature distorted tetrahedral geometries and the GaN_2C_3 rings adopt the typical *boat-type* conformation. The Ga–Si bond length (2.4471(19) Å) is comparable to those of **1–3** and other compounds with Ga–Si single bonds (2.33–2.53 Å).[21] The Ga–Si–Ga bond angle (126.16(8)°) is larger than the ideal tetrahedral angle and clearly reflects the repulsive interactions between the sterically demanding L(Br)Ga substituents. The Si–NH_2 (1.716(6) Å) bond lengths agree with those previously reported for these type of compounds (Si–N 1.729(1) Å,[18a] 1.711(3) Å, 1.703(3) Å[18b] 1.653(3) Å,[18c] 1.691(4) Å[18d]).

To further investigate the role of the X substituents on the bonding nature of these types of silylene carbonyl complexes, we performed quantum chemical computations. We optimized the silylene carbonyl complexes with different atoms or groups attached to Ga: X = F, Cl, Br, I, Me, OMe, NMe_2. All DFT computations were carried out using B3LYP[22] with Grimme's D3BJ dispersion correction,[23] as implemented in Gaussian16 revision C.01.[24] The 6-311G(d,p) basis set was used for all atoms except Ga, I and Br, for which the def2-TZVP[25] basis set was employed. All minima were characterized with analytical Hessian calculations to ensure minima (*i.e.*, no imaginary frequencies). NBO analyses were performed with NBO 7.0[26] as implemented in Gaussian16.

Our computations suggest that the electronic effect of the substituent X on the C–O bond length is rather small. However, while the differences between the different halogen atoms are negligible, electron donating groups such as Me, OMe, NMe_2 slightly shorten the Si–C bond and increase the C–O bond length (Table 2). This is reflected by the bond lengths, Wiberg bond orders and by the computed IR shifts for the C–O bond. Our computed C–O bond lengths somewhat differ from experiment since the computed C–O bond in **3** is longer than in **I** (matches experiment) and **2** (unlike experiment). However, the computed trends in the IR $\nu_{C=O}$ match the experimental trends.

Wiberg bond indices suggest that the Ga–X bond is weaker than a single bond, and the bond order increases with decreasing electronegativity along F, O < N < C, and increases when going down the halogen series F < Cl < Br < I. The bonds further away from the X group are less affected by electronegativity, as for Me, OMe, and NMe_2 the Si–C bond order is higher and the C–O bond lower relative to the other groups. From these results the most significant change in $\nu_{C=O}$, in

Table 1 Selected bond lengths and angles of silylene carbonyl complexes **2**, **3**, **I**, and **II**

	$[L(I)Ga]_2SiCO$ **2**	$[L(Me)Ga]_2SiCO$ **3**	$[L(Br)Ga]_2SiCO$ **I**	$[(Me_3Si)_3Si]({}^tBu_3Si)SiCO$ **II**
Ga–Si [Å]	2.4230(8), 2.4348(9)	2.4314(4), 2.4213(4)	2.4204(5)	—
Si–C [Å]	1.808(2)	1.770(2)	1.865(6)	1.794(2)
C–O [Å]	1.149(3)	1.144(2)	1.136(7)	1.153(2)
Ga–X [Å]	2.6012(5), 2.5840(5)	1.990(2), 1.992(2)	2.3777(3)	—
Ga–Si–Ga [°]	119.22(3)	116.10(2)	122.73(4)	—
Si–C–O [°]	172.2(2)	170.8(2)	172.7(6)	171.3(1)

Table 2 Computed data (at the B3LYP-D3BJ level of theory with a def2-TZVP for Ga, Br, I and 6-311G(d,p) for all other atoms) for $[L(x)Ga]_2Si$: –CO complexes, and their RMSD from the crystal structure

X=	*F*	Cl	Br	Br **I** (exp.)	I	I **2** (exp.)	Me	Me **3** (exp.)	OMe	NMe_2
RMSD			0.533		0.414		0.364			
r_{Ga-X}[a]	1.815	2.228	2.382	2.3777(3)	2.595	2.6012(5) 2.5840(5)	2.001	1.9898(13) 1.9923(14)	1.836	1.873
r_{Ga-Si}[a]	2.437	2.437	2.440	2.4203(5)	2.441	2.4230(7) 2.4348(7)	2.439	2.4213(4) 2.4314(4)	2.419	2.436
r_{Si-C}	1.815	1.811	1.811	1.865(6)	1.811	1.808(3)	1.791	1.7703(18)	1.804	1.790
r_{C-O}	1.150	1.151	1.151	1.136(7)	1.151	1.149(3)	1.157	1.144(2)	1.153	1.156
$\angle_{Ga-Si-Ga}$	111.9	113.0	113.9	122.73(4)	115.0	119.22(3)	116.0	116.105(16)	108.4	122.9
$\angle_{Ga-Si-C}$[a]	88.9	90.2	90.6	92.97(15)	91.0	90.81(7) 91.02(8)	92.4	95.16(5) 94.13(5)	90.6	91.6
$\angle_{Si-C-O}$	171.7	171.2	171.0	172.7(6)	170.8	172.2(2)	171.3	170.82(19)	169.8	171.9
$\angle_p$[b]	88.0	90.3	91.0		91.9		94.61		91.0	93.4
WBI_{Ga-R}[c]	0.43	0.67	0.75		0.84		0.60		0.43	0.48
WBI_{Ga-Si}[c]	0.79	0.81	0.81		0.82		0.79		0.80	0.80
WBI_{Si-C}[c]	1.30	1.29	1.29		1.28		1.36		1.33	1.36
$WBI_{C=O}$[c]	2.02	2.01	2.02		2.02		1.95		1.98	1.95
$\nu_{C=O}$[d]	1966	1959	1958	1945	1956	1934	1925	1906	1946	1934
HOMO[e]	−5.50	−5.53	−5.48		−5.42		−4.91		−5.34	−4.88
LUMO[e]	−1.37	−1.41	−1.44		−1.51		−1.22		−1.27	−1.18

[a] Average value of the two bonds. [b] Pyramidalization angle, as measured from the angle between the Si–C bond and the centroid of the two Ga atoms. [c] WBI, Wiberg bond index. [d] Scaled with a factor of 0.967. [e] Orbital energies in eV.

bond lengths and in bond orders is a reduction observed for electron donating groups (either inductively or resonatively) such as X = Me and NMe_2. Interestingly, OMe has a very similar influence. The $\nu_{C=O}$ vibration correlates well with σ_F[27] (Fig. 2), and thus operates as a measure of field/inductive effects of the groups. σ_F matches the F parameter presented in Table I of ref. 27*b*.

Field/inductive effects are long range through-space or through-bond dipolar interactions, different from the short-range effect of electronegativity. As this effect arises from dipole interactions and can roughly be related to the size of the dipole moment,[27a] we can rationalize this as the interaction between the Ga–X and the Si–C–O dipole moments. A larger $Ga^{\delta+}$–$X^{\delta-}$ dipole moment would interact more favorably with a smaller $C^{\delta+}$–$O^{\delta-}$ dipole moment. Free CO has a small dipole moment of 0.107 D,[28] pointing towards the carbon atom (*i.e.*, $^{\delta-}CO^{\delta+}$) while carbonyls with C–O double bonds have larger dipole moments (with the partial negative charge on oxygen).

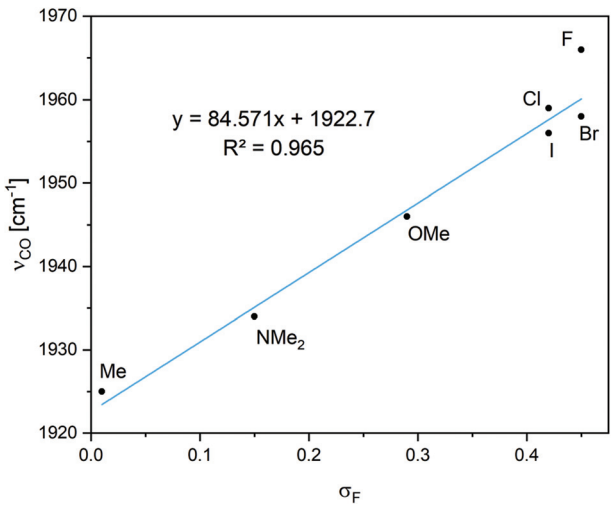

Fig. 2 The correlation between $\nu_{C=O}$ and the field inductive effects of the various groups (σ_F).[27b]

This would suggest that larger $Ga^{\delta+}$–$X^{\delta-}$ dipole moments would destabilize the longer, more polar C–O bonds, resulting in shorter bonds. Alternatively, this can be explained by considering the π-back-donation of electrons from silicon, which is expected to result in larger dipole moments pointing towards the oxygen, being destabilized as the $Ga^{\delta+}$–$X^{\delta-}$ dipole moment becomes larger. This concept has also been reported from other groups.[29] However, the orbital interaction energies from second order perturbation theory analysis do not show a good correlation with σ_F, suggesting a more complex orbital picture (Table S2†). Also, in contrast to the field/inductive effect, the $\nu_{C=O}$ vibration does not show good correlations with measurements of resonance interactions (see ESI for details†).[27b]

The HOMO of all complexes is a bonding orbital between the Si atom's lone pair and the π^*_{CO} (Fig. S25†). Table 2 shows that for X = Me and NMe_2 both HOMO and LUMO are slightly higher in energy than for the other complexes, indicating that the Si–C–O unit is more electron rich. This can be also observed from the NBO charges (Table S2†), showing a more negative charge on the CO for X = Me, NMe_2, OMe. Hirshfeld charges (Table S3†) show a similar picture. Note that for both charge partitioning methods the charge on the silicon does not follow the electronegativity order (NBO charge is the most negative for F > Cl > Br > I for example) or the electron donation/withdrawal ability (very similar NBO charges for Me, OMe, NMe_2), or the field effect.

Table S2† also shows the results of second order perturbation theory for the interaction energies between the orbitals. Both the $LP_{Si} \rightarrow \pi^*_{CO}$ and $\sigma_{Si-Ga} \rightarrow \pi^*_{CO}$ interactions give gener-

ally higher values for X = Me, NMe_2, and OMe than for the halogens, in accordance with the longer C–O bond length for the electron donating groups. However, no such correlation between the electron donating groups, or between the different halogen substitutents was observed. To conclude, our computations demonstrate that groups attached to the Ga atoms have only relatively small effects on the Si–C and C–O bond lengths. These groups do not interact *via* resonance with the SiCO unit, but instead their main influence is through field/inductive interactions.

Conclusions

Two new room-temperature stable silylene carbonyl complexes $[L(X)Ga]_2SiCO$ (X = I **2**, Me **3**) were synthesized and structurally characterized by single crystal X-ray diffraction. Quantum chemical computations were employed to analyze the influence of different substituents X on the electronic nature of the complexes and the strength of the π backbonding interaction from the silylene to the carbonyl ligand, hence resulting in different Si–CO bond strengths and, consequently, different activities of $[L(X)Ga]_2SiCO$ with respect to small molecule activations. This was revealed in several reactions including those with ammonia, in which only $[L(Br)Ga]_2SiCO$ **I** was found to undergo oxidative addition of the N–H bond with subsequent formation of $[L(X)Ga]_2Si(H)NH_2$ **4**, whereas $[L(Me)Ga]_2SiCO$ **3** failed to react.

The halide-substituted carbonyl complex **I** turned out to be more reactive than the Me-substituted complex **3**. To increase the reactivity of such silylene carbonyl complexes, the Si–CO bond needs to be weakened, which can be achieved by hampering the π-backbonding contribution of the silylene. The synthesis of heteroleptic silylenes containing only one electropositive L(X)Ga and one electronegative ligand, *i.e.*, β-diketiminate or amidinate substituent, might therefore be a promising strategy.

Experimental

General procedures

All manipulations were performed in an atmosphere of purified argon using standard Schlenk and glove-box techniques. NMR-scale reactions were carried out in *J*-Young NMR tubes. *n*-Hexane was dried using mBraun Solvent Purification System (SPS). Benzene was dried over potassium. Deuterated solvents were dried over activated molecular sieves (4 Å) and degassed prior to use. The anhydrous nature of the solvents was verified by Karl Fischer titration. LGa {L = HC[C(Me)N(2,6-^{i}Pr$_2$C$_6$H$_3$)]$_2$},[30] $[L(Br)Ga]_2SiCO$[13] and ^{Dipp}NHC-SiI$_4$[31] were prepared according to literature methods and other chemicals were obtained from commercial sources and purified prior to use in necessary cases. Microanalyses were performed at the elemental analysis laboratory of University of Duisburg-Essen. Melting points were measured using a Thermo Scientific 9300 apparatus.

^{1}H (300.1 MHz; 400 MHz),^{13}C{^{1}H} (75.5 MHz; 101 MHz) and ^{29}Si{^{1}H} (59.1 MHz; 79 MHz) NMR spectra were recorded using a Bruker Avance DPX-300 spectrometer or AscendTM 400 spectrometer. ^{1}H and ^{13}C{^{1}H} spectra were referenced to internal C_6D_5H (^{1}H: δ = 7.154; ^{13}C: δ = 128.39), while ^{29}Si{^{1}H} NMR and ^{29}Si spectra were referenced using IUPAC recommendation of NMR nomenclature.[32] IR spectra were recorded with an ALPHA-T FT-IR spectrometer equipped with a single reflection ATR sampling module, which was placed in a glovebox to guarantee measurements under inert gas conditions.

Synthesis procedures

Synthesis of {[L(I)Ga]Si[Ga(I)][CHC(Me)NAr][C(Me)NAr]} 1. LGa (300 mg, 0.616 mmol) and DippNHC-SiI$_4$ (0.190 g, 0.205 mmol) were dissolved in cold toluene (3 mL, −30 °C), slowly warmed to room temperature and stirred for 1 d. Concentration of the resulting solution to 2 mL and storage at 4 °C for 3 d gave yellow crystals of {[L(I)Ga]Si[Ga(I)][CHC(Me)NAr][C(Me)NAr]} **1**. The crystals were filtered, washed with 0.4 mL of cold benzene, and finally dried *in vacuo*.

Yield: 0.162 mg (0.129 mmol, 63%). M.p. 188–189 °C (dec.). Anal. Calcd for $C_{58}H_{82}N_4I_2Ga_2Si$: C, 55.44; H, 6.58; N, 4.46. Found: C, 55.49; H, 6.63; N, 4.41%. IR (neat): ν 2961, 2922, 2866, 1517, 1461, 1437, 1386, 1362, 1314, 1251, 1200, 1176, 1128, 1100, 1052, 1021, 933, 866, 838, 802, 766, 715, 632, 524, 501, 425 cm^{-1}. ^{1}H NMR (C_6D_6, 300.1 MHz): δ 7.14–6.94 (m, 12 H, $C_6H_3(^iPr)_2$), 5.03 (s, 1 H, γ-C*H*), 4.57 (s, 1 H, Si–C*H*═), 4.11 (sept, $^3J_{HH}$ = 6.6 Hz, 1 H, C*H*(CH$_3$)$_2$), 3.82 (sept, $^3J_{HH}$ = 6.9 Hz, 1 H, C*H*(CH$_3$)$_2$), 3.56 (sept, $^3J_{HH}$ = 6.9 Hz, 1 H, C*H*(CH$_3$)$_2$), 3.47 (sept, $^3J_{HH}$ = 6.6 Hz, 1 H, C*H*(CH$_3$)$_2$), 3.30 (sept, $^3J_{HH}$ = 6.9 Hz, 1 H, C*H*(CH$_3$)$_2$), 3.14 (sept, $^3J_{HH}$ = 6.9 Hz, 1 H, C*H*(CH$_3$)$_2$), 2.91 (sept, $^3J_{HH}$ = 6.9 Hz, 1 H, C*H*(CH$_3$)$_2$), 2.53 (sept, $^3J_{HH}$ = 6.9 Hz, 1 H, C*H*(CH$_3$)$_2$), 1.82 (s, 3 H, SiCHC(C*H*$_3$)NAr), 1.59 (d, $^3J_{HH}$ = 6.6 Hz, 3 H, CH(C*H*$_3$)$_2$), 1.54 (m, 15 H, CH(C*H*$_3$)$_2$, ArNCC*H*$_3$), 1.38 (d, $^3J_{HH}$ = 6.6 Hz, 3 H, CH(C*H*$_3$)$_2$), 1.28 (s, 3 H, SiC(C*H*$_3$)NAr), 1.24 (d, $^3J_{HH}$ = 6.6 Hz, 3 H, CH(C*H*$_3$)$_2$), 1.23 (d, $^3J_{HH}$ = 6.6 Hz, 3 H, CH(C*H*$_3$)$_2$), 1.19 (d, $^3J_{HH}$ = 6.9 Hz, 6 H, CH(C*H*$_3$)$_2$), 1.14 (d, $^3J_{HH}$ = 6.6 Hz, 3 H, CH(C*H*$_3$)$_2$), 1.08 (d, $^3J_{HH}$ = 6.9 Hz, 3 H, CH(C*H*$_3$)$_2$), 1.04 (d, $^3J_{HH}$ = 6.9 Hz, 3 H, CH(C*H*$_3$)$_2$), 1.01 (d, $^3J_{HH}$ = 6.9 Hz, 3 H, CH(C*H*$_3$)$_2$), 0.95 (d, $^3J_{HH}$ = 6.6 Hz, 3 H, CH(C*H*$_3$)$_2$), 0.94 (d, $^3J_{HH}$ = 6.6 Hz, 3 H, CH(C*H*$_3$)$_2$), 0.85 (d, $^3J_{HH}$ = 6.9 Hz, 3 H, CH(C*H*$_3$)$_2$). ^{13}C NMR (C_6D_6, 75.5 MHz): δ 170.1 (ArN*C*CH$_3$), 169.6 (SiCH*C*(*C*H$_3$)NAr), 168.1 (Si*C*(*C*H$_3$)NAr), 147.1, 146.6, 146.5, 146.4, 143.6, 143.0, 142.5, 142.4, 141.9, 141.8, 141.5, 141.4, 140.9, 128.3, 128.1, 127.3, 126.2, 126.0, 125.6, 124.7, 124.6, 123.9, 123.8, 123.7 (*C*$_6$H$_3$), 99.2 (γ-*C*H), 85.7 (–Si–*C*H═), 30.2, 29.5, 29.2, 28.7, 28.2, 27.9, 27.8, 27.6 (*C*H(CH$_3$)$_2$), 27.4, 27.2, 26.7, 26.6, 25.8, 25.7, 25.5, 25.1, 25.0, 24.9, 24.9, 24.8, 24.7, 24.5, 24.4, 24.2 (CH(*C*H$_3$)$_2$), 24.1 (ArNC*C*H$_3$), 23.9 (SiCHC(*C*H$_3$)NAr), 23.6 (SiC(*C*H$_3$)NAr). ^{29}Si NMR (C_6D_6, 59.6 MHz): δ −31.9.

Synthesis of $[L(I)Ga]_2SiCO$ (2). A dissolved mixture of LGa (150 mg, 0.308 mmol) and ^{Dipp}NHC-SiI$_4$ (94.8 mg, 0.103 mmol) in frozen benzene (1 mL, −30 °C) was charged with CO gas (1 atm). The reaction mixture was stirred at room temperature for 1 d to afford a red solution, which was concen-

trated to 0.5 mL and stored at 4 °C for 24 h, yielding orange crystals of $[L(I)Ga]_2SiCO$ **2**. The crystals were filtered, washed with 0.5 mL of benzene, and dried *in vacuo*.

Yield: 91 mg (0.071 mmol, 69%). M.p. 168–169 °C (dec.). Anal. Calcd for $C_{59}H_{82}N_4I_2Ga_2OSi$: C, 55.16; H, 6.43; N, 4.36. Found: C, 55.90; H, 6.49; N, 4.21%. IR (neat): ν 2961, 2922, 2862, 1934, 1528, 1461, 1434, 1382, 1319, 1255, 1176, 1100, 1021, 937, 858, 794, 759, 640, 576, 532, 505, 438 cm^{-1}. ^1H NMR (C_6D_6, 300.1 MHz): δ 7.14–6.96 (m, 12 H, $C_6H_3(^iPr)_2$), 5.02 (s, 2 H, γ-C*H*), 3.85 (sept, $^3J_{HH}$ = 6.9 Hz, 4 H, C*H*$(CH_3)_2$), 3.20 (sept, $^3J_{HH}$ = 6.9 Hz, 4 H, C*H*$(CH_3)_2$), 1.48 (s, 12 H, ArNCC*H*$_3$), 1.35 (d, $^3J_{HH}$ = 6.6 Hz, 12 H, CH(C*H*$_3)_2$), 1.25 (d, $^3J_{HH}$ = 6.9 Hz, 12 H, CH(C*H*$_3)_2$), 1.21 (d, $^3J_{HH}$ = 6.9 Hz, 12 H, CH(C*H*$_3)_2$), 0.96 (d, $^3J_{HH}$ = 6.9 Hz, 12 H, CH(C*H*$_3)_2$). ^{13}C NMR (C_6D_6, 75.5 MHz): δ 207.0 (Si*C*O), 169.4 (ArN*C*CH$_3$), 146.6, 142.9, 141.7, 127.7, 125.9, 123.8 (C_6H_3), 99.0 (γ-*C*H), 30.4, 29.7 (*C*H$(CH_3)_2$), 28.6, 25.2, 24.4, 24.3 (CH(*C*H$_3)_2$), 24.1 (ArNC*C*H$_3$). ^{29}Si NMR (C_6D_6, 59.6 MHz): δ −249.9.

Synthesis of $[L(Me)Ga]_2SiCO$ (3). A mixture of $[L(Br)Ga]_2SiCO$ **I** (100 mg, 0.084 mmol) and MeLi (1.85 mg, 0.084 mmol) were dissolved in toluene (1 mL) and stirred at room temperature for 2 d. The solution was concentrated to 0.5 mL and stored at 4 °C for 24 h, yielding orange crystals of $[L(Me)Ga]_2SiCO$ **3**.

Yield: 56.2 mg (0.053 mmol, 63%). M.p. 249 °C (dec.). Anal. Calcd for $C_{59}H_{82}N_4I_2Ga_2OSi$: C, 69.06; H, 8.36; N, 5.28. Found: C, 68.7; H, 8.48; N, 5.33%. IR (neat): ν 3060, 2958, 2925, 2868, 1942, 1906, 1549, 1517, 1435, 1383, 1314, 1254, 1177, 1100, 1017, 935, 855, 794, 757, 697, 636, 536, 444 cm^{-1}. ^1H NMR (C_6D_6, 400 MHz): δ 7.15–6.97 (m, 12 H, $C_6H_3(^iPr)_2$), 4.76 (s, 2 H, γ-C*H*), 3.44 (sept, $^3J_{HH}$ = 6.8 Hz, 4 H, C*H*$(CH_3)_2$), 3.17 (sept, $^3J_{HH}$ = 6.8 Hz, 4 H, C*H*$(CH_3)_2$), 1.47 (s, 12 H, ArNCC*H*$_3$), 1.34 (d, $^3J_{HH}$ = 6.8 Hz, 12 H, CH(C*H*$_3)_2$), 1.18 (d, $^3J_{HH}$ = 6.8 Hz, 12 H, CH(C*H*$_3)_2$), 1.10 (d, $^3J_{HH}$ = 6.8 Hz, 12 H, CH(C*H*$_3)_2$), 1.07 (d, $^3J_{HH}$ = 6.8 Hz, 12 H, CH(C*H*$_3)_2$), 0.32 (s, 6 H, GaC*H*$_3$). ^{13}C NMR (C_6D_6, 101 MHz): δ 207.5 (Si*C*O), 168.0 (ArN*C*CH$_3$), 144.6 (N*C*C(CH$(CH_3)_2$)), 143.2, 143.0 (NC*C*(CH$(CH_3)_2$)), 126.8, 124.4, 124.1 (C_6H_3), 96.7 (γ-*C*H-), 29.4 (*C*H$(CH_3)_2$), 27.7 (CH(*C*H$_3)_2$), 27.6 (*C*H$(CH_3)_2$), 25.2, 24.3, 24.2, (CH(*C*H$_3)_2$), 24.2 (ArNC*C*H$_3$), −0.26 (Ga*C*H$_3$). ^{29}Si NMR (C_6D_6, 79 MHz): δ −285.2.

Synthesis of $[L(Br)Ga]_2Si(H)NH_2$ (4). A solution of $[L(Br)Ga]_2SiCO$ **I** (100 mg, 0.084 mmol) in 2 mL of toluene was frozen and the atmosphere was removed. The solution was warmed up to −20 °C, charged with dry ammonia (dried over sodium) and stirred for 15 minutes at −20 °C and 15 min at room temperature, upon the color of solution changed from orange/red to colorless. The solvent was removed *in vacuo* and 0.8 mL of *n*-hexane was added. The solution was filtered and stored at −18 °C to give colorless crystals of $[L(Br)Ga]_2Si(H)NH_2$ **4**.

Yield: 42.4 mg (0.036 mmol, 43%). M.p. 189 °C (dec.). Anal. Calcd for $C_{58}H_{85}Br_2Ga_2N_5Si$: C, 59.05; H, 7.24; N, 5.94. Found: C, 59.58; H, 6.92; N, 4.73%. IR (neat): ν 3428, 3345, 3127, 3020, 2953, 2859, 2060, 1520, 1453, 1430, 1377, 1311, 1254, 1172, 1100, 1016, 937, 856, 794, 756, 668, 625, 534, 442 cm^{-1}. ^1H NMR (C_6D_6, 400 MHz): δ 7.15–6.97 (m, 12 H, $C_6H_3(^iPr)_2$), 4.96 (s, 2 H, γ-C*H*), 4.67 (t, $^3J_{HH}$ = 4.6 Hz, 1H, Si*H*), 3.94 (sept, $^3J_{HH}$ = 6.7 Hz, 2 H, C*H*$(CH_3)_2$), 3.67 (sept, $^3J_{HH}$ = 6.7 Hz, 2 H, C*H*$(CH_3)_2$), 3.23 (sept, $^3J_{HH}$ = 6.7 Hz, 4 H, C*H*$(CH_3)_2$), 1.54 (s, 6 H, ArNCC*H*$_3$), 1.51 (s, 6 H, ArNCC*H*$_3$), 1.42 (d, $^3J_{HH}$ = 6.6 Hz, 6 H, CH(C*H*$_3)_2$), 1.30 (d, $^3J_{HH}$ = 6.8 Hz, 6 H, CH(C*H*$_3)_2$), 1.23 (d, $^3J_{HH}$ = 6.6 Hz, 6 H, CH(C*H*$_3)_2$), 1.21 (d, $^3J_{HH}$ = 6.8 Hz, 6 H, CH (C*H*$_3)_2$), 1.20 (d, $^3J_{HH}$ = 6.8 Hz, 6 H, CH(C*H*$_3)_2$), 1.13 (d, $^3J_{HH}$ = 6.8 Hz, 6 H, CH(C*H*$_3)_2$), 0.98 (d, $^3J_{HH}$ = 6.8 Hz, 12 H, CH (C*H*$_3)_2$), −1.67 (d, $^3J_{HH}$ = 4.4 Hz, 2 H, SiN*H*$_2$). ^{13}C NMR (C_6D_6, 101 MHz): δ 168.8 (ArN*C*CH$_3$), 147.0, 146.2 (N*C*C(CH$(CH_3)_2$)), 143.2, 143.0, 142.3, 141.5 (NC*C*(CH$(CH_3)_2$)), 127.5, 127.3, 125.6, 125.4, 123.4, 123.4 (C_6H_3), 98.6 (γ-*C*H), 29.7 (*C*H$(CH_3)_2$, 29.4, 29.2, 28.7 (CH(*C*H$_3)_2$), 28.4, 28.0 (*C*H$(CH_3)_2$, 25.2, 24.9, 24.6, 24.2, 24.0 (CH(*C*H$_3)_2$), 23.8, 23.7(ArNC*C*H$_3$), 23.3 (CH (*C*H$_3)_2$). ^{29}Si NMR (C_6D_6, 119 MHz, DEPT90): −39.6 ($^1J_{HSi}$ = 175.6 Hz).

Data availability

All additional data part of the ESI.†

Author contributions

J. S. and C. G. performed the experiments, E. S. the quantum chemical calculations, C. W. the single crystal X-ray diffraction. The work was supervised by St. S. and P. R. S. The manuscript was written through contributions of all authors. All authors have given approval to the final version of the manuscript.

Conflicts of interest

There are no conflicts to declare.

Acknowledgements

We acknowledge financial support from the Deutsche Forschungsgemeinschaft DFG (St. S., SCHU 1069/26-1), the University of Duisburg-Essen (St. S.), the Justus Liebig University (P. R. S.), and the Alexander-von-Humboldt-Foundation (Fellowship to E. S.).

Notes and references

1 (*a*) P. P. Power, *Nature*, 2010, **463**, 171–177; (*b*) C. Weetman and S. Inoue, *ChemCatChem*, 2018, **10**, 4213–4228; (*c*) R. L. Melen, *Science*, 2019, **363**, 479–484.
2 (*a*) M. Asay, C. Jones and M. Driess, *Chem. Rev.*, 2011, **111**, 354–396; (*b*) C. Shan, S. Yao and M. Driess, *Chem. Soc. Rev.*, 2020, **49**, 6733–6754.
3 (*a*) S. Yadav, S. Saha and S. S. Sen, *ChemCatChem*, 2016, **8**, 468–501; (*b*) T. J. Hadlington, M. Driess and C. Jones, *Chem. Soc. Rev.*, 2018, **47**, 4176–4197.

4 (*a*) N. Wiberg, *Lehrbuch der Anorganischen Chemie*, De Gruyter, Berlin, Boston, 2008; (*b*) S. Fuhimori and S. Inoue, *J. Am. Chem. Soc.*, 2022, **144**, 2034–2050.

5 (*a*) X. Wu, L. Zhao, D. Jiang, I. Fernández, R. Berger, M. Zhou and G. Frenking, *Angew. Chem., Int. Ed.*, 2018, **57**, 3974–3980; (*b*) X. Wu, L. Zhao, J. Jin, S. Pan, W. Li, X. Jin, G. Wang, M. Zhou and G. Frenking, *Science*, 2018, **361**, 912–916; (*c*) C. R. Landis, R. P. Hughes and F. Weinhold, *Science*, 2019, **365**, 2355; (*d*) L. Zhao, S. Pan, M. Zhou and G. Frenking, *Science*, 2019, **365**, 5021; (*e*) Q. Zhang, W.-L. Li, C.-Q. Xu, M. Chen, M. Zhou, J. Li, D. M. Andrada and G. Frenking, *Angew. Chem., Int. Ed.*, 2015, **54**, 11078–11083.

6 (*a*) J. C. Jeffery, N. C. Norman, J. A. J. Pardoe and P. L. Timms, *Chem. Commun.*, 2000, 2367–2368; (*b*) M. Finze, E. Bernhardt, A. Terheiden, M. Berkei, H. Willner, D. Christen, H. Oberhammer and F. Aubke, *J. Am. Chem. Soc.*, 2002, **124**, 15385–15398; (*c*) J. D. Glore, J. W. Rathke and R. Schaeffer, *Inorg. Chem.*, 1973, **12**, 2175–2178.

7 (*a*) H. Braunschweig, R. D. Dewhurst, F. Hupp, M. Nutz, L. Radacki, C. W. Tate, A. Vargas and Q. Ye, *Nature*, 2015, **522**, 327–330; (*b*) M. Rang, F. Fantuzzi, M. Arrowsmith, E. Beck, R. Witte, A. Matler, A. Rempel, T. Bischof, K. Radacki, B. Engels and H. Braunschweig, *Angew. Chem., Int. Ed.*, 2021, **60**, 2963–2968.

8 (*a*) A. Stoy, M. Härterich, R. D. Dewhurst, J. O. C. Jiménez-Halla, P. Endres, M. Eyßelein, T. Kupfer, A. Deissenberger, T. Thiess and H. Braunschweig, *J. Am. Chem. Soc.*, 2022; (*b*) A. Hofmann, M.-A. Légaré, L. Wüst and H. Braunschweig, *Angew. Chem., Int. Ed.*, 2019, **58**, 9776–9781; (*c*) H. Braunschweig, I. Krummenacher, M.-A. Légaré, A. Matler, K. Radacki and Q. Ye, *J. Am. Chem. Soc.*, 2017, **139**, 1802–1805.

9 F. F. Puschmann, D. Stein, D. Heift, C. Hendriksen, Z. A. Gal, H.-F. Grützmacher and H. Grützmacher, *Angew. Chem., Int. Ed.*, 2011, **50**, 8420–8423.

10 Phosphaketenes of p-block elements: Group 13: (*a*) M. K. Sharma, C. Wölper, G. Haberhauer and S. Schulz, *Angew. Chem., Int. Ed.*, 2021, **60**, 6784; (*b*) D. Wilson, W. Myers and J. M. Goicoechea, *Dalton Trans.*, 2020, **49**, 15249–15255; (*c*) D. W. N. Wilson, M. P. Franco, W. K. Myers, J. E. McGrady and J. M. Goicoechea, *Chem. Sci.*, 2020, **11**, 862–869; (*d*) W. Yang, K. E. Krantz, D. A. Dickie, A. Molino, D. J. D. Wilson and R. J. Gilliard, *Angew. Chem., Int. Ed.*, 2020, **59**, 3971–3975; (*e*) Y. Mei, J. E. Borger, D. J. Wu and H. Grützmacher, *Dalton Trans.*, 2019, **48**, 4370–4374. Group 14: (*f*) S. Yao, Y. Xiong, T. Szilvási, H. Grützmacher and M. Driess, *Angew. Chem., Int. Ed.*, 2016, **55**, 4781–4785; (*g*) Y. Xiong, S. Yao, T. Szilvási, E. Ballestero-Martínez, H. Grützmacher and M. Driess, *Angew. Chem., Int. Ed.*, 2017, **56**, 4333–4336; (*h*) S. Bestgen, M. Mehta, T. C. Johnstone, P. W. Roesky and J. M. Goicoechea, *Chem. Eur. J.*, 2020, **26**, 9024–9031. Group 15: (*i*) Z. Li, X. Chen, M. Bergeler, M. Reiher, C. Y. Su and H. Grützmacher, *Dalton Trans.*, 2015, **44**, 6431–6438; (*j*) L. Liu, D. A. Ruiz, D. Munz and G. A. Bertrand, *Chem.*, 2016, **1**, 147–153; (*k*) Z. Li, X. Chen, L. Liu, D. A. Ruiz, J. L. Peltier, G. Bertrand, C.-Y. Su and H. Grützmacher, *Angew. Chem., Int. Ed.*, 2016, **55**, 6018–6022; (*l*) M. M. Hansmann, D. A. Ruiz, L. Liu, R. Jazzar and G. Bertrand, *Chem. Sci.*, 2017, **8**, 3720–3725.

11 (*a*) V. Lavallo, Y. Canac, B. Donnadieu, W. W. Schoeller and G. Bertrand, *Angew. Chem., Int. Ed.*, 2006, **45**, 3488–3491; (*b*) C. Goedecke, M. Leibold, U. Siemeling and G. Frenking, *J. Am. Chem. Soc.*, 2011, **133**, 3557–3569.

12 (*a*) R. R. Lembke, R. F. Ferrante and W. Weltner, Jr., *J. Am. Chem. Soc.*, 1977, **99**, 416–423; (*b*) R. S. Grev and H. F. Schaefer III, *J. Am. Chem. Soc.*, 1989, **111**, 5687–5691; (*c*) M. Zhou, L. Jiang and Q. Xu, *J. Chem. Phys.*, 2004, **121**, 10474–10482; (*d*) G. Maier, H. P. Reisenauer and H. Egenolf, *Organometallics*, 1999, **18**, 2155–2161; (*e*) C. A. Arrington, J. T. Petty, S. E. Payne and W. C. K. Haskins, *J. Am. Chem. Soc.*, 1988, **110**, 6240–6241; (*f*) M. A. Pearsall and R. West, *J. Am. Chem. Soc.*, 1988, **110**, 7228–7229; (*g*) M. Tacke, C. Klein, A. J. Stufkens, A. Oskam, P. Jutzi and E. A. Bunte, *Z. Anorg. Allg. Chem.*, 1993, **619**, 865–868; (*h*) H. Bornemann and W. Sander, *J. Organomet. Chem.*, 2002, **641**, 156–164.

13 C. Ganesamoorthy, J. Schoening, C. Wölper, L. Song, P. R. Schreiner and S. Schulz, *Nat. Chem.*, 2020, **12**, 608–614.

14 D. Reiter, R. Holzner, A. Porzelt, P. Frisch and S. Inoue, *Nat. Chem.*, 2020, **12**, 1131–1135.

15 T. Sergeieva, D. Mandal and D. M. Andrada, *Chem. – Eur. J.*, 2021, **27**, 10601–10609.

16 A. Kempter, C. Gemel and R. A. Fischer, *Inorg. Chem.*, 2008, **47**, 7279–7285.

17 C. Helling, C. Ganesamoorthy, C. Wölper and S. Schulz, *Dalton Trans.*, 2022, **51**, 2050–2058.

18 (*a*) A. V. Protchenko, J. I. Bates, L. M. A. Saleh, M. P. Blake, A. D. Schwarz, E. L. Kolychev, A. L. Thompson, C. Jones, P. Mountford and S. Aldridge, *J. Am. Chem. Soc.*, 2016, **138**, 4555–4564; (*b*) T. J. Hadlington, J. A. B. Abdalla, R. Tirfoin, S. Aldridge and C. Jones, *Chem. Commun.*, 2016, **52**, 1717–1720; (*c*) A. Jana, C. Schulzke and H. W. Roesky, *J. Am. Chem. Soc.*, 2009, **131**, 4600–4601; (*d*) N. Weyer, M. Heinz, J. I. Schweizer, C. Bruhn, M. C. Holthausen and U. A. Siemeling, *Angew. Chem., Int. Ed.*, 2021, **60**, 2624–2628; (*e*) D. Reiter, R. Holzner, A. Porzelt, P. J. Altmann, P. Frisch and S. Inoue, *J. Am. Chem. Soc.*, 2019, **141**, 13536–12546.

19 D. Reiter, P. Frisch, D. Wendel, F. M. Hörmann and S. Inoue, *Dalton Trans.*, 2020, **49**, 7060–7068.

20 R. C. Fischer and P. P. Power, *Chem. Rev.*, 2010, **110**, 3877–3923.

21 Search for Ga–Si single bonds in the CSD gave 86 hits ranging from 2.3290 Å to 2.5360 Å (mean 2.442 Å). C. R. Groom, I. J. Bruno, M. P. Lightfoot and S. C. Ward, Acta Cryst., 2016, **B72**, 171–179.

22 (*a*) A. D. Becke, *J. Chem. Phys.*, 1993, **98**, 5648–5652; (*b*) C. Lee, W. Yang and R. G. Parr, *Phys. Rev. B*, 1988, **37**, 785–789.

23 S. Grimme, S. Ehrlich and L. Goerigk, *J. Comput. Chem.*, 2011, **32**, 1456–1465.

24 M. J. Frisch, G. W. Trucks, H. B. Schlegel, G. E. Scuseria, M. A. Robb, J. R. Cheeseman, G. Scalmani, V. Barone, G. A. Petersson, H. Nakatsuji, X. Li, M. Caricato, A. V. Marenich, J. Bloino, B. G. Janesko, R. Gomperts, B. Mennucci, H. P. Hratchian, J. V. Ortiz, A. F. Izmaylov, J. L. Sonnenberg, D. Williams-Young, F. Ding, F. Lipparini, F. Egidi, J. Goings, B. Peng, A. Petrone, T. Henderson, D. Ranasinghe, V. G. Zakrzewski, J. Gao, N. Rega, G. Zheng, W. Liang, M. Hada, M. Ehara, K. Toyota, R. Fukuda, J. Hasegawa, M. Ishida, T. Nakajima, Y. Honda, O. Kitao, H. Nakai, T. Vreven, K. Throssell, J. A. Montgomery, Jr., J. E. Peralta, F. Ogliaro, M. Bearpark, J. J. Heyd, E. N. Brothers, K. N. Kudin, V. N. Staroverov, T. A. Keith, R. Kobayashi, J. Normand, K. Raghavachari, A. P. Rendell, J. C. Burant, S. S. Iyengar, J. Tomasi, M. Cossi, J. M. Millam, M. Klene, C. Adamo, R. Cammi, J. W. Ochterski, R. L. Martin, K. Morokuma, O. Farkas, J. B. Foresman and D. J. Fox, *Gaussian 16 (Revision C.01)*, Gaussian, Inc., Wallingford CT, 2016.

25 F. Weigend and R. Ahlrichs, *Phys. Chem. Chem. Phys.*, 2005, **7**, 3297–3305.

26 (*a*) E. D. Glendening, J. K. Badenhoop, A. E. Reed, J. E. Carpenter, J. A. Bohmann, C. M. Morales, P. Karafiloglou, C. R. Landis and F. Weinhold, *NBO Version 7.0; TCI*, University of Wisconsin, Madison, WI, 2018; (*b*) E. D. Glendening, C. R. Landis and F. Weinhold, *Comput. Mol. Sci.*, 2012, **2**, 1–42.

27 (*a*) R. W. Taft and R. D. Topsom, The Nature and Analysis of Substitutent Electronic Effects, in *Progress in Physical Organic Chemistry*, John Wiley & Sons, Ltd, 1987, pp. 1–83; (*b*) C. Hansch, A. Leo and R. W. Taft, *Chem. Rev.*, 1991, **91**, 165–195.

28 G. Tsankova, M. Richter, P. L. Stanwix, E. F. May and R. Span, *ChemPhysChem*, 2018, **19**, 784–792. Other calculated and experimental values can be found in this reference.

29 (*a*) N. S. Hush and M. L. Williams, *J. Mol. Spectrosc.*, 1974, **50**, 349–368; (*b*) A. S. Goldman and K. Krogh-Jespersen, *J. Am. Chem. Soc.*, 1996, **118**, 12159–12166; (*c*) G. Bistoni, S. Rampino, N. Scafuri, G. Ciancaleoni, D. Zuccaccia, L. Belpassi and F. Tarantelli, *Chem. Sci.*, 2013, **7**, 1174–1184.

30 N. J. Hardman, B. E. Eichler and P. P. Power, *Chem. Commun.*, 2000, 1991–1992.

31 A. C. Filippou, Y. N. Lebedev, O. Chernov, M. Straßmann and G. Schnakenburg, *Angew. Chem., Int. Ed.*, 2013, **52**, 6974–6978.

32 R. K. Harris, E. D. Becker, S. M. Cabral de Menezes, R. Goodfellow and P. Granger, *Magn. Reson. Chem.*, 2002, **40**, 489–505.